Nonlinear Phenomena in Complex Systems, vol. **27**, no. 4 (2024), pp. 386 - 397

Tenth-order QED Corrections to the Lepton Anomaly Due to Some Bubble Diagrams

O. P. Solovtsova,[1, 2, *] V. I. Lashkevich,[1, †] and L. P. Kaptari[2, ‡]

[1] *Gomel State Technical University, Gomel, 246746, BELARUS*

[2] *Bogoliubov Laboratory of Theoretical Physics, Joint Institute for Nuclear Research, Dubna, Moscow Region, 141980 RUSSIA*

(Received 28 September, 2024)

Analytical expressions for the tenth-order mass-dependent radiative corrections to the lepton anomaly of each of the charged leptons are derived explicitly for a certain class of QED Feynman diagrams with insertions of the vacuum polarization operator with four closed lepton loops, where only one loop consists of leptons ℓ different from the external leptons L, $\ell \neq L$. The approach is based on the consecutive application of dispersion relations for the photon polarization operator and of the Mellin–Barnes transform of the propagators of massive particles. The result is expressed in terms of the mass ratio $r = m_\ell/m_L$. We investigate the behaviour of the exact analytical expressions as $r \to 0$ and $r \to \infty$ and compare it with the corresponding asymptotic expansions known in the literature. We assert that in the region of physical values of r the asymptotic expansions provide a high precision approximation to the exact results.

PACS numbers: 13.40.Em, 12.20.Ds, 14.60.Ef

Keywords: anomalous magnetic moment of leptons, Mellin–Barnes representation, Feynman diagrams, electromagnetic vacuum-polarization contributions

DOI: https://doi.org/10.5281/zenodo.14508985

1. Introduction

The electromagnetic self interaction of charged spin 1/2 point-like particles (leptons) shifts the gyromagnetic factor g_L from the value 2, predicted by the Dirac's theory [1], $g_L \neq 2$, leading to the famous effect referred in the literature to as the anomalous magnetic moment of leptons defined as $a_L = (g_L - 2)/2$. This effect is of a great importance in understanding the physics of the Standard Model (SM) and beyond; consequently a plenty of nowadays high precision experiments is devoted to measurements of a_L of leptons, $L = e$, μ and τ The accuracy of the measurements is of the order of 0.1 parts per trillion (ppt) for electrons [2, 3] and 0.20 parts per million (ppm) for muons [4]. This imposes corresponding improvements of the accuracy of theoretical calculations within the SM and even investigations of physics of possible effects beyond the SM. The accuracy of experiments requires theoretical calculations for the radiative corrections of the order of α^5 or higher, where $\alpha = e^2/4\pi$ is the fine structure constant, see, e.g., Ref. [5]. Due to the complexities of analytical calculations of so high order corrections, one usually employs numerical methods [6–9] with involvements of specific computational algorithms that allow for high precision numerical manipulations, e.g., the known PSLQ algorithm [10]. However, these numerical calculations are rather computer-time consuming, the corresponding codes are quite lengthy and, consequently, independent confirmation of the results is difficult. Hence, it appears tempting to find at least a class of some specific Feynman diagrams that can be calculated analytically and the obtained explicit expressions to be used in cross-checking of the

* E-mail: `solovtsova@gstu.gomel.by;olsol@theor.jinr.ru`

† E-mail: `lashkevich@gstu.gomel.by`

‡ E-mail: `kaptari@theor.jinr.ru`

numerical results. Moreover, explicit analytical results will allow for separate detailed analysis of different partial contributions. This is the subclass of diagrams known as the "bubble"-like diagrams which consist on the lepton electromagnetic vertex with insertions of the photon vacuum polarization operators with solely closed lepton loops.

Among the first analytical calculations of the "bubble"-like diagrams of the eighth-order and tenth-order QED contributions to the muon anomaly, one can mention Ref. [11] where computations were performed within a framework with combined utilization of the dispersion relations and Mellin–Barnes transform. Earlier, the Mellin–Barnes formalism was suggested in Ref. [12] to be used as a tool for evaluating the massive Feynman integrals. This technique is quite popular and widely used in the literature in multi-loop calculations in the relativistic quantum field theories, cf. Refs. [13–15]. In Ref. [11] analytical expressions for a_μ was presented as an expansion in terms of the ratio $r = m_\ell/m_L$, where m_L is the mass of the external lepton L, and m_ℓ is the mass of the internal leptons $\ell \neq L$ in the loops of the polarization operator. The eighth-order and tenth-order QED corrections in Ref. [11] were calculated as asymptotic expansions of the ratio r at low $r \ll 1$ and high $r \gg 1$ for the muon anomaly. The approach was generalized in Ref. [16] to any kind of leptons where exact expressions for corrections with all possible combinations of the external L and internal ℓ leptons, $L = e$, μ and τ, in the whole interval of the ratio $0 < r < \infty$ were presented. The eighth order corrections from three-loop diagrams with all possible combinations of leptons L and ℓ were given in Ref. [16]. The diagrams with four identical loops ($\ell\ell\ell\ell$) were analysed in Ref. [17]; the ones with two loops L and two loops ℓ, i.e. the diagrams of the type ($LL\ell\ell$), were presented in Ref. [18], while the ($L\ell\ell\ell$) diagrams – in Ref. [19]. In the present paper we focus on the tenth order coefficients $A_2^{(10))}(r)$ for the particular class of four-loop diagrams with only one internal lepton ℓ different from the external lepton L, i.e., for the ($LLL\ell$) diagrams, as depicted in Fig. 1. We deduce analytical expressions for the ($LLL\ell$) corrections of $A_2^{(10))}(r)$ in the whole interval of r for all types of leptons L and ℓ. To be able to compare our results with the ones previously reported in the literature, we perform asymptotic expansions at $r \to 0$ and $r \to \infty$ and investigate their validity for the ratio r_{phys} corresponding to the physically existing lepton masses. We argue that it suffices to consider only few first terms in the asymptotic expansions to calculate $A_2^{(10))}(r)$ at r_{phys} with the desired accuracy.

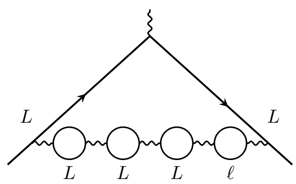

FIG. 1: Tenth-order diagram considered in the present paper. The values of p and j in Eq. (1) are $p = 3$ and $j = 1$.

2. Basic formulae

The herein section is dedicated to the consideration of the most general form of the QED corrections to the lepton anomalous magnetic moment due to bubble-like Feynman diagrams with insertions of the photon polarization operator with an arbitrary number $n = p + j$ of lepton loops, where p is the number of loops consisting of leptons L of the same type as the external one, and j denotes the leptons $\ell \neq L$. The corresponding Feynman diagram is depicted in Fig. 2, left panel.

It is straightforward to show [11, 16, 20]) that by applying consecutively the dispersion relations to the polarization operators and the Mellin–Barnes representation [12–14] for the Feynman parametric integrals, the electromagnetic vertex $\Gamma_\mu(p_1, p_2)$ of the $(n+1)$-th order, left panel in Fig. 2, can be related to the vertex diagram of the second order with exchanges of one but massive photon, as

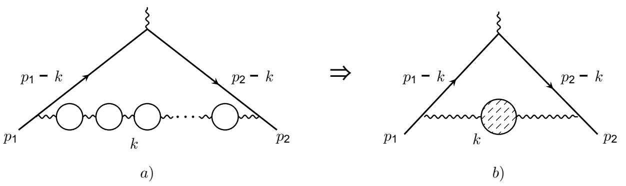

FIG. 2: The Feynman diagrams considered in this paper contributing to the lepton anomalous magnetic moment. Left panel: radiative corrections to the electromagnetic lepton vertex with insertions of the vacuum polarization operator with an arbitrary number n of lepton loops. Right panel: the second order diagram representing the set of graphs depicted in the left panel as exchanges of one massive photon, see text.

depicted in the right panel of Fig. 2. Then the general expressions for the radiative corrections corresponding to bubble-like diagrams with $n = p + j$ closed lepton loops can be written as (see Refs. [11, 16] for details)

$$a_L(p,j) = \frac{\alpha}{\pi}\frac{1}{2\pi i}F_{(p,j)}\int\limits_{c-i\infty}^{c+i\infty} dz\ \left(\frac{4m_\ell^2}{m_L^2}\right)^{-z} \times \Gamma(z)\Gamma(1-z)\left(\frac{\alpha}{\pi}\right)^j R_j(z)\left(\frac{\alpha}{\pi}\right)^p \Omega_p(z). \tag{1}$$

In Eq. (1) $F_{(p,j)} = (-1)^{p+j+1}C^p_{p+j}$ where C^p_{p+j} are the familiar binomial coefficients; the variable c is an arbitrary number from the interval $a < \mathrm{Re}\, z < b$ that defines the z-strip of the analyticity of the integrand (1). The Mellin momenta $R_j(z)$ and $\Omega_p(z)$ in Eq. (1) are determined by the polarization operators $\Pi^{(L)}$ and $\Pi^{(\ell)}$ according to

$$\left(\frac{\alpha}{\pi}\right)^j R_j(z) = \int\limits_0^\infty \frac{dy}{y}\left(\frac{4m_\ell^2}{y}\right)^z \frac{1}{\pi}\mathrm{Im}\left[\Pi^{(\ell)}(y)\right]^j, \tag{2}$$

$$\left(\frac{\alpha}{\pi}\right)^p \Omega_p(z) = \int\limits_0^1 dx\, x^{2z}(1-x)^{1-z} \times\left[\Pi^{(L)}\left(-\frac{x^2}{1-x}m_L^2\right)\right]^p, \tag{3}$$

The explicit expressions for $\Pi^{(L,\ell)}$ in Eqs. (3) and (2) are well known in the literature, q.v. Ref. [20]

$$\mathrm{Re}\,\Pi^{(L,\ell)}(y) = \left(\frac{\alpha}{\pi}\right)\left[\frac{8}{9} - \frac{\delta^2}{3} + \delta\left(\frac{1}{2} - \frac{\delta^2}{6}\right) \times \ln\frac{|1-\delta|}{1+\delta}\right],$$

$$\frac{1}{\pi}\mathrm{Im}\,\Pi^{(L,\ell)}(y) = \left(\frac{\alpha}{\pi}\right)\delta\left(\frac{1}{2} - \frac{\delta^2}{6}\right)\theta\left(y - 4m^2_{(L,\ell)}\right),$$

where $\delta = \sqrt{1 - 4m^2_{(L,\ell)}/y}$. Evidently, since the operator $\Pi^{(L)}\left(-\frac{x^2}{1-x}m_L^2 < 0\right)$ in Eq. (3) is of the Euclidean nature, and since the θ-function in $\mathrm{Im}\,\Pi^{(L,\ell)}(y)$, the polarization operator $\Pi^{(L)}\left(-\frac{x^2}{1-x}m_L^2\right)$ is purely real and does not depend on the lepton masses,

$$\Pi^{(L)}\left(-\frac{x^2}{1-x}m_L^2\right) = \frac{\alpha}{\pi}\left[\frac{5}{9} + \frac{4}{3x} - \frac{4}{3x^2} + \left(-\frac{1}{3} + \frac{2}{x^2} - \frac{4}{3x^3}\right)\ln(1-x)\right]. \tag{4}$$

Furthermore, by a simple change of variables, $y = 4m_\ell^2/\xi$ in Eq. (2), it is straightforward to show that $R_j(z)$ is also independent of the lepton masses. Consequently, the only dependence of a_L in Eq. (1) on masses enters through the ratio

$$r = \frac{m_\ell}{m_L}. \tag{5}$$

This variable is commonly accepted in the literature to classify the contributions to a_L from different Feynman diagrams; it allows to emphasize separately terms completely independent of masses, the so-called universal contribution A_1 at $r = 1$ and the mass-dependent terms $A_2(r)$ and $A_3(r_1, r_2)$ at $r \neq 1$ (for details, see Ref. [5]):

$$a_L = A_1\left(\frac{m_L}{m_L}\right) + A_2\left(\frac{m_\ell}{m_L}\right) + A_3\left(\frac{m_{\ell_1}}{m_L}, \frac{m_{\ell_2}}{m_L}\right). \tag{6}$$

At the same time, each term in Eq. (6) can be represented as Taylor expansions over the fine structure constant α, i.e.

$$A_1(r=1) = A_1^{(2)}\left(\frac{\alpha}{\pi}\right)^1 + A_1^{(4)}\left(\frac{\alpha}{\pi}\right)^2 + \\ + A_1^{(6)}\left(\frac{\alpha}{\pi}\right)^3 + A_1^{(8)}\left(\frac{\alpha}{\pi}\right)^4 + A_1^{(10)}\left(\frac{\alpha}{\pi}\right)^5 + \cdots, \tag{7}$$

$$A_2(r) = A_2^{(4)}(r)\left(\frac{\alpha}{\pi}\right)^2 + A_2^{(6)}(r)\left(\frac{\alpha}{\pi}\right)^3 \\ + A_2^{(8)}(r)\left(\frac{\alpha}{\pi}\right)^4 + A_2^{(10)}(r)\left(\frac{\alpha}{\pi}\right)^5 + \cdots, \tag{8}$$

$$A_3(r_1,r_2) = A_3^{(6)}(r_1,r_2)\left(\frac{\alpha}{\pi}\right)^3 \\ + A_3^{(8)}(r_1,r_2)\left(\frac{\alpha}{\pi}\right)^4 + A_3^{(10)}(r_1,r_2)\left(\frac{\alpha}{\pi}\right)^5 + \cdots, \tag{9}$$

where $r_1 = m_{\ell_1}/m_L$, $r_2 = m_{\ell_2}/m_L$, with $m_{\ell_{1,2}}$ as masses of two internal leptons $\ell_{1,2}$ different from L. The leading order contribution to a_L was obtained, for the first time, by Schwinger [21], $a_L \simeq \alpha/2\pi$, which, in our notation, corresponds to $A_1^{(2)} = 1/2$. The universal coefficients A_1 were further studied analytically in a series of publications (see, e.g., Refs. [22, 23]) where explicit expressions were found for a rather high order n, up to $n = 13$. It is also worth mentioning that the coefficients $A_1^{(2n)}$ decrease for $n < 7$ and, starting from $n = 7$, increase factorially.

The analytical behaviour of the mass-dependent coefficients $A_{2,3}$ for high enough n ($n > 4$) remains hitherto unstudied. So far, higher-order analysis has been based mainly on either approximate asymptotic expansion of the corresponding Feynman diagrams or more accurate but cumbersome and computer time consuming numerical calculations.

It turns out that the analytical expressions for $A_2^{(2n+2)}(r)$ are quite cumbersome; therefore in testing the consistency of the final results, one often employs thorough comparisons of the limits $A_2^{(2n+2)}(r \to 1)$ with the well-known analytic expression for $A_1^{(2n+2)}(1)$, see e.g. Refs. [23, 24]. In our case

$$A_1^{(10)} = -\frac{3689383}{656100} - \frac{21928\,\pi^4}{1403325} - \frac{128\,\zeta(3)}{675} \\ + \frac{64\,\zeta(5)}{9} \approx 4.7090571603... \times 10^{-4}. \tag{10}$$

It is also instructive to stress that the universal coefficient of the previous order $2n+2$ with $n = 1, 2, 3$, i.e., $A_1^{(4,6,8)}(1)$ can be immediately obtained from Eq. (3) as the Mellin momenta $\Omega_{n=1,2,3}(z)$ at $z = 0$.

3. Analytical calculations

In this Section we proceed with explicit calculations of the diagram in Fig. 1, for which $p = 3$, $j = 1$ and, consequently $F_{(p,j)} = -4$. Then Eqs. (1) and (8) entail that

$$A_2^{(10)LLL\ell}(r) = -\frac{4}{2\pi i}\int\limits_{c-i\infty}^{c+i\infty} (4r^2)^{-z}\Gamma(z)\Gamma(1-z) \\ \times R_1(z)\Omega_3(z)dz, \tag{11}$$

where the Mellin momenta $R_1(z)$ and $\Omega_3(z)$, see Eqs. (2) and (3), read as

$$R_1(z) = \frac{\sqrt{\pi}}{4}\,\frac{\Gamma(2+z)}{z\,\Gamma(5/2+z)} \tag{12}$$

and

$$
\begin{aligned}
\Omega_3(z) = {} & \frac{125}{729}X_0(z,0) - \frac{64}{27}X_0(z,-6) + \frac{64}{9}X_0(z,-5) - \frac{112}{27}X_0(z,-4) - \frac{32}{9}X_0(z,-3) + \frac{140}{81}X_0(z,-2) \\
& + \frac{100}{81}X_0(z,-1) - \frac{25}{81}X_1(z,0) - \frac{64}{9}X_1(z,-7) + + \frac{224}{9}X_1(z,-6) - \frac{608}{27}X_1(z,-5) - \frac{160}{27}X_1(z,-4) \\
& + \frac{908}{81}X_1(z,-3) + \frac{14}{9}X_1(z,-2) - \frac{40}{27}X_1(z,-1) + \frac{5}{27}X_1(z,0) - \frac{64}{9}X_2(z,-8) + \frac{256}{9}X_2(z,-7) \\
& - \frac{928}{27}X_2(z,-6) + \frac{32}{9}X_2(z,-5) + \frac{140}{9}X_2(z,-4) - \frac{104}{27}X_2(z,-3) - \frac{8}{3}X_2(z,-2) + \frac{4}{9}X_2(z,-1) \\
& - \frac{1}{27}X_3(z,0) - \frac{64}{27}X_3(z,-9) + \frac{32}{3}X_3(z,-8) - 16X_3(z,-7) + \frac{56}{9}X_3(z,-6) + \frac{16}{3}X_3(z,-5) \\
& - 4X_3(z,-4) - \frac{4}{9}X_3(z,-3) + \frac{2}{3}X_3(z,-2),
\end{aligned}
\tag{13}
$$

where we introduced the following notation:

$$
X_k(z,n) = \int_0^1 dx x^{2z+n}(1-x)^{1-z}\ln^k(1-x). \tag{14}
$$

Integrals (14) can be carried out explicitly with the result

$$
\begin{aligned}
X_0(z,n) &= \frac{\Gamma(2-z)\Gamma(1+n+2z)}{\Gamma(3+n+z)}, \\
X_1(z,n) &= X_0(z,n)\Big(\psi\,(2-z) - \psi\,(3+n+z)\Big) \\
X_2(z,n) &= X_0(z,n)\Bigg[\Big(\psi\,(2-z) - \psi\,(3+n+z)\Big)^2 \\
&+ \psi^{(1)}\,(2-z) - \psi^{(1)}\,(3+n+z)\Bigg], \\
X_3(z,n) &= X_0(z,n)\Bigg\{\Big[\psi(2-z) - \psi(3+n+z)\Big]^3 \\
&+ 3\Big[\psi(2-z) - \psi(3+n+z)\Big] \\
&\times \Big[\psi^{(1)}(2-z) - \psi^{(1)}(3+n+z)\Big] \\
&+ \psi^{(2)}(2-z) - \psi^{(2)}(3+n+z)\Bigg\},
\end{aligned}
\tag{15}
$$

where $\psi(x)$, $\psi^{(1)}(x)$ and $\psi^{(2)}(x)$ are the polygamma functions of the order 0, 1 and 2, respectively.

As mentioned, the universal coefficient of the previous order $2n+2$ with $n = 1,2,3$, i.e. $A_1^{(4,6,8)}(1)$ can be immediately obtained from Eq. (3) as the Mellin momenta $\Omega_{n=1,2,3}(z)$ at $z = 0$. So, the eighth order coefficients are (cf. Ref. [16])

$$
A_1^{(8)} = -\lim_{z\to 0}\Omega_3(z) = \frac{151849}{40824} - \frac{2}{45}\pi^4 + \frac{32}{63}\zeta(3), \tag{16}
$$

which is nothing but the exact analytical expression for $A_1^{(8)}$ known in the literature, see, e.g., Ref. [23]. Above, in Eq. (16), $\zeta(3)$ is the Euler-Riemann zeta function.

Further, using Eqs. (12)-(15) one can rearrange Eq. (11) to obtain a more compact form of the coefficients $A_L^{(10)LLL\ell}(r)$

$$
A_L^{LLL\ell}(r) = -\frac{4}{2\pi i}\int\limits_{c-i\infty}^{c+i\infty} r^{-2z}\mathcal{F}(z)dz, \tag{17}
$$

where the integrand $\mathcal{F}(z)$ reads as

$$
\begin{aligned}
\mathcal{F}(z) = {} & \Bigg\{ -\frac{zQ_1(z) + \pi^2\left(2+3z+z^2\right)^2 Q_2(z)}{2(z-4)(z-3)(z-2)(z-1)} \\
& \times \frac{(2z-7)(2z-5)}{z(z+1)^3(z+2)^3} - \Bigg[\frac{\pi\, Q_3(z)}{3(z-1)z(z+1)^2(z+2)^2} \\
& - 54(-35+4z+47z^2-24z^3+3z^4)\psi^{(1)}(-z)\Bigg]\cot(\pi z) \\
& + \frac{Q_4(z)\psi^{(1)}(-z)}{(z-4)(z-3)(z-2)(z-1)z(z+1)(z+2)}\Bigg\} \\
& \times \frac{2\pi^2}{9Z(z)\sin(\pi z)^2}.
\end{aligned}
\tag{18}
$$

In Eq. (18) $Q_{1-4}(z)$ are the polynomials and the function $Z(z)$ in the denominator looks like

$$Z(z) = z\,(z+2)(2z-7)(2z-5)(2z-3)(2z-1) \times (2z+1)(2z+3). \qquad (19)$$

From Eqs. (18) and (19), one immediately infers that the integrand $\mathcal{F}(z)$ in (17) is a singular function in the complex plane of z with numerous poles of different orders originating from the zeros of the denominator of $\mathcal{F}(z)$ and from singularities of the functions $\cot(\pi z)$ and $\psi^{(1)}(z)$. The higher-order residues we calculated by means of a symbol manipulation package such as the "Wolfram Mathematica" or "Maple" program systems with built-in libraries allowing analytical symbolic calculations. Then the integral (17) can be calculated by the Cauchy residue theorem by closing the integration contour consecutively in the right ($r > 1$) and left ($r < 1$) semiplanes of the complex variable z. Below, along with the variable r, we widely use the variable $t = r^2$, that facilitates comparisons of our results with the corresponding expressions well-known in the literature.

a. **The left semiplane:** $r < 1$. By closing the contour of integration to the left and computing the corresponding residues in this domain, we get the following result

$$A_2^{(10)LLL\ell}(r<1) = C_0(r) + C_1(r)\ln(r^2) + C_2(r)\ln^2(r^2) + \Sigma_1(r). \qquad (20)$$

The expressions of $C_{0,1,2}(r)$ turned out to be lengthy, containing a number of Euler-Riemann zeta functions, polylogarithms $\mathrm{Li}_{n=2,3,4,5}(r)$, therefore we do not present them here, limiting ourselves to the expansions derived from them.

The last term in Eq. (20) is the remaining part of the sum over residues, which cannot be summed as finite expressions with solely ordinary or special functions,

$$\Sigma_1(r) = \frac{8}{9}\sum_{n=5}^{\infty}\Big\{\big[U_1(n) + U_2(n)\ln(r^2) - U_3(n)\ln^2(r^2)\big]\,\psi^{(1)}(n) + \big[U_2(n) - 2U_3(n)\ln(r^2)\big]\psi^{(2)}(n) - U_3(n)\psi^{(3)}(n)\Big\} r^{2n}\,, \qquad (21)$$

where the polynomials $U_{i=1,2,3}$ read as

$$\begin{aligned}U_1(n) = {}& (1296243648000 + 3554725305600n - 16506863523360n^2 - 54634993591968n^3 \\ & + 79126014733992n^4 + 352709519700528n^5 - 21529000412568n^6 - 958012707066648n^7 \\ & - 502985408885851n^8 + 1316237550535538n^9 + 1304567835267877n^{10} - 886363099366492n^{11} \\ & - 1648029022182067n^{12} - 49464155746630n^{13} + 1088581912544723n^{14} + 531281976591752n^{15} \\ & - 273553914249634n^{16} - 336240959851264n^{17} - 60349526763400n^{18} + 65799427846016n^{19} \\ & + 41856942836864n^{20} + 5240522170112n^{21} - 4168609708288n^{22} - 2258398984192n^{23} \\ & - 465273541120n^{24} - 14273536000n^{25} + 14816827392n^{26} + 3699474432n^{27} + 425967616n^{28} \\ & + 24969216n^{29} + 589824n^{30}) \,/\, \big[(n-1)^2(n+1)^2(2+n)^2(3+n)^2(4+n)^2 Y_1(n)^3\big]\,, \end{aligned} \qquad (22)$$

$$
\begin{aligned}
&U_2(n) = -(57153600 + 84732480n - 617507604n^2 - 914732964n^3 + 1374291015n^4 + 2544708862n^5 \\
&- 796452257n^6 - 3105687569n^7 - 907980806n^8 + 1321227379n^9 + 987930424n^{10} + 41071472n^{11} \\
&- 194849344n^{12} - 81652576n^{13} - 9384640n^{14} + 1995776n^{15} + 727040n^{16} + 80640n^{17} + 3072n^{18}) \\
&/ \left[(n-1)(n+1)(2+n)(3+n)(4+n)Y_1(n)^2\right], \\
&U_3(n) = 27\left(-35 - 4n + 47n^2 + 24n^3 + 3n^4\right)/Y_1(n), \qquad (23)\\
&Y_1(n) = (7+2n)(5+2n)(3+2n)(2n-1)(1+2n)(-3+2n)(n-2)n.
\end{aligned}
$$

b. **The right semiplane:** $r > 1$ In the same manner, we calculate and sum up all the residues in the right semiplane of z. The result is presented in the form

$$
\begin{aligned}
&A_2^{(10),LLL\ell}(r > 1) = D_0(r) + D_1(r)\ln(r^2) \\
&+ D_2(r)\ln^2(r^2) + D_3(r)\ln^3(r^2) + D_4(r)\ln^4(r^2) \\
&+ \Sigma_2(r) \qquad (24)
\end{aligned}
$$

with the sum $\Sigma_2(r)$ determined by the same quantities $U_{1,2,3}$ and $\psi^{(1,2,3)}$ as in $\Sigma_1(r)$, Eq. (21),

$$
\begin{aligned}
\Sigma_2(r) = \frac{8}{9}\sum_{n=5}^{\infty}\Bigg\{ &\left[U_1(-n) + U_2(-n)\ln(r^2) - U_3(-n)\times\ln^2(r^2)\right]\psi^{(1)}(n) - \left[U_2(-n) - 2U_3(-n)\ln(r^2)\right] \\
&\times\psi^{(2)}(n) - U_3(-n)\psi^{(3)}(n)\Bigg\}\frac{1}{r^{2n}}. \qquad (25)
\end{aligned}
$$

As before, the last term $\Sigma_2(r)$ in Eq. (24) arises from the remaining part of the sum over residues in the right semiplane $r > 1$ which cannot be summed up in a close analytical form with purely ordinary and/or special functions.

4. Asymptotical expansions

The obtained formulae for the coefficients $A_2^{LLL\ell}(r)$ determine entirely the behavior of the corresponding corrections in both left, $r < 1$, Eq. (20), and right semiplanes, $r > 1$, Eq. (24). Due to cumbersomeness of the analytical expressions, a thorough numerical analysis of $A_2^{LLL\ell}(r)$ appears to be substantially hindered and rather awkward in practical application. However, qualitative investigations of $A_2^{LLL\ell}(r)$ can be essentially relieved if, instead of the exact analytical formulae, one employs their asymptotic expansions at low, $r \ll 1$, and large, $r \gg 1$, values of the ratio of the lepton masses. Such analyzes have been widely used in the literature [11]. It should be noted that at physical values of the lepton masses the ratio r is basically located namely in these regions; actually in the right semiplane $r_{phys} > 16 \gg 1$ whereas in the left semiplane $r_{phys} < 0.06 \ll 1$, see [25]. Here below we present separate analysis of the asymptotic of $A_2^{LLL\ell}(r)$ in the left and right semiplanes, respectively. To this end and to simplify comparisons with the results reported previously in the literature, we use the variable $t = r^2$ instead of r. However, the final pictures are presented again in terms of r which emphasize more clearly the main peculiarities of the lepton anomalies as functions of their masses.

c. **Left semiplane: $t < 1$.** We expand the coefficients $A_2^{(10),LLL\ell}(t = r^2)$, Eq. (20), in the left semiplane keeping terms up to t^4. The result is

$$
\begin{aligned}
A^{(10),LLL\ell}_{2\ asymp.}(t \ll 1) =& -\frac{46796257}{3214890} + \frac{143}{81}\pi^2 + \frac{124}{8505}\pi^4 + \left(-\frac{151849}{30618} + \frac{8}{135}\pi^4 - \frac{128}{189}\zeta(3)\right)\ln t \\
&+ \left(\frac{92476}{6615} - \frac{16}{9}\pi^2\right)\zeta(3) + \left(-\frac{374711}{45927} - \frac{16}{675}\pi^2 + \frac{16}{405}\pi^4 + \frac{2144}{567}\zeta(3)\right)t \\
&+ \left[\frac{16107486427}{70020304200} + \frac{5260603}{26790750}\pi^2 - \frac{11504}{467775}\pi^4 + \left(-\frac{1565849}{5051970} - \frac{16}{525}\pi^2 + \frac{8}{405}\pi^4 - \frac{34064}{31185}\zeta(3)\right)\ln t\right. \\
&\left.+ \left(\frac{652419088}{108056025} - \frac{16}{27}\pi^2\right)\zeta(3)\right]t^2 + \frac{1}{25}\left[\frac{20439596209}{26296514244} + \frac{41112361}{11252115}\pi^2 - \frac{1448}{11583}\pi^4 - \frac{1673428808}{81162081}\zeta(3)\right. \\
&\left.+ \left(-\frac{932795}{312741} - \frac{21964}{35721}\pi^2 + \frac{28960}{3861}\zeta(3)\right)\ln t\right]t^3 + \frac{1}{25}\left[\frac{22028123510917}{5259302848800} - \frac{1152406}{50426145}\pi^2 - \frac{601}{27027}\pi^4\right. \\
&\left.+ \frac{4}{45}\ln t^2 - \frac{72554936}{81162081}\zeta(3) + \left(-\frac{423448433}{145945800} + \frac{4493}{29106}\pi^2 + \frac{12020}{9009}\zeta(3)\right)\ln t\right]t^4 + \mathcal{O}\left(t^5\right). \qquad (26)
\end{aligned}
$$

We compare our expansion (26) with the corresponding expression reported in Ref. [11], where the expansion was restricted up to terms $\mathcal{O}(t^3)$ (cf. Eq. (B7) of Ref. [11]). We found that with this accuracy the two explicit expressions perfectly reconcile with each other. Albeit, we shall stress that our definition of $\Omega_3(z)$ slightly differs from the one reported in Ref. [11]. Note also that since summation in (21) starts from $n = 5$, the sum $\Sigma_1(r)$ do not contribute to the expansion Eq. (26).

Results of exact numerical calculations by Eq. (20) (solid line) together with the approximate results by the asymptotic formula (26) (dashed and dotted lines) are presented in Fig. 3. It demonstrates that in the region $r < 0.4$ the exact and approximate results practically coincide. Surprisingly, at $r > 0.4$ the expansion $\sim \mathcal{O}(r^6)$ approximates the exact results much better (the deviation being maximum $\sim 7\%$ at $r \to 1$) than the expansion that includes the next order in r. Moreover, a remarkable circumstance here is that accounting for the next terms up to $\sim \mathcal{O}(r^{10})$ in the asymptotic expansion, the results diverge drastically from the exact ones at larger r. Evidently, since up to terms $\sim \mathcal{O}(r^{10})$ the sum $\Sigma_1(r)$ does not contribute to (26), this is a direct indication of the role of higher orders in r in the expansion (20) and, presumably, points on the increasing role of $\Sigma_1(r)$ at larger r, especially at $r \to 1$. This can be better understood if one splits the exact result for $A_2^{(10)LLL\ell}(r < 1)$ into two parts, one containing all the terms from (20) except for the sum $\Sigma_1(r)$, the second one as properly the sum $\Sigma_1(r)$:

$$A_2^{(10)LLL\ell}(r < 1) = \mathcal{P}(r) + \Sigma_1(r). \qquad (27)$$

Then the asymptotic expansion (26) corresponds to expansion of $\mathcal{P}(r)$ up to $\sim \mathcal{O}(r^{10})$ which, as seen from Fig. 3, is quite justified in the interval $(0 < r < 0.5)$. With increase of r, more and more terms are required to be kept in the expansion.

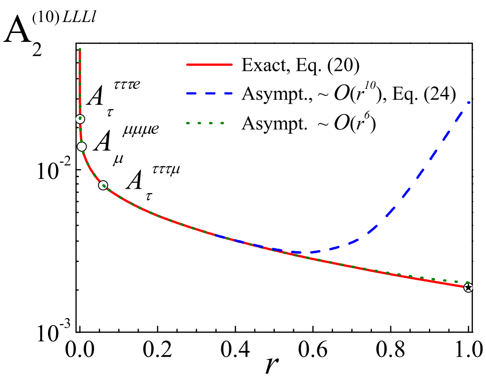

FIG. 3: The tenth order corrections $A_2^{(10)LLL\ell}(r \leq 1)$ in the left semiplane, $r \leq 1$. The solid line is the result of full calculations by Eq. (20), the dotted line corresponds to the asymptotic expansion keeping terms up to $\sim \mathcal{O}(r^6)$; the dashed line corresponds to the asymptotic expansion (26) keeping terms up to $\sim \mathcal{O}(r^{10})$. The open circles, as well as the associated with them labels, point to the coefficients $A_2^{(10),LLL\ell}(r)$ at r corresponding to physical values of the lepton masses. The star indicates the value of the mass independent coefficient $4A_1^{(10),LLL\ell}(r = 1)$, see Eq. (10).

This clearly exhibits the Fig. 4, where the relative contributions of the $\mathcal{P}(r)$ and $\Sigma_1(r)$ to the exact corrections $A_2^{(10)LLL\ell}(r < 1)$ are presented. It demonstrates that the term $\mathcal{P}(r)$ dominates in the interval $(0 < r < 0.7)$ then its contribution decreases rather fast. At first glance, there is a discrepancy in behaviour of the asymptotic of $\mathcal{P}(r)$ in Fig. 3, which is always above the exact values of $A_2^{(10)LLL\ell}(r < 1)$, and the contribution of the exact $\mathcal{P}(r)$, which imposes a behaviour below the exact $A_2^{(10)LLL\ell}(r < 1)$ (compare the dashed lines in Figs. 3 and 4). Obviously, such an apparent contradiction is merely a clear evidence that the asymptotic expansion $r \ll 1$ becomes inapplicable at $r > 0.5 \div 0.6$. However, in practice one focus on the interval $r < 0.06$, where all the physical values of r are located, see Fig. 3. Consequently, the approximate expression (26) can be safely used for concrete estimates of $A_2^{(10)LLL\ell}(r < 0.06)$. The accuracy of such approximate calculations can be estimated if one defines the relative deviation of the asymptotic expressions from the exact ones as

$$\varepsilon(r) = \frac{\left| A_{2\ \mathrm{exact}}^{(10)\ LLL\ell}(r) - A_{2\ \mathrm{asymp.}}^{(10)\ LLL\ell}(r) \right|}{A_{2\ \mathrm{exact}}^{(10)\ LLL\ell}(r)} \qquad (28)$$

and computes ε for different values of r. So, calculations based on the expansion $\sim \mathcal{O}(r^6)$ performed in the physical interval of lepton masses at $r < 1$ ranges from $\varepsilon(r) \sim 5 \cdot 10^{-22}$ at $r = 2.88 \cdot 10^{-4}$ (corresponds $\approx m_e/m_\tau$) to $\varepsilon(r) \sim 2 \cdot 10^{-8}$ at $r = 0.0594$ (corresponds to $\approx m_\mu/m_\tau$).

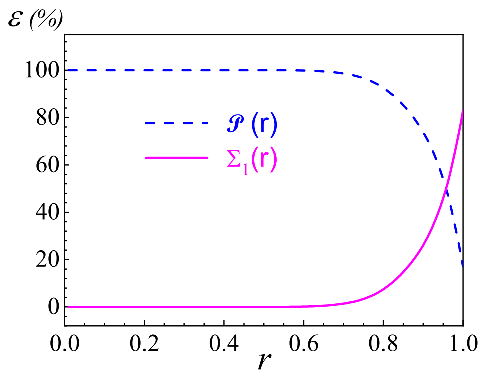

FIG. 4: The relative contribution of the two terms in Eq. (27) to the corrections $A_2^{(10)LLL\ell}(r < 1)$. The solid line is the contribution of $\Sigma_1(r)$ and the dashed line is the contribution of $\mathcal{P}(r)$.

d. **Right semiplane:** $t > 1$. Analogous calculations in the right semiplane up to terms $\mathcal{O}\left(1/t^5\right)$ give

$$
\begin{aligned}
A^{(10)}_{2,as}(t) \underset{t\gg 1}{=} & \left(\frac{202991}{656100} - \frac{4}{2025}\pi^4 - \frac{64}{675}\,\zeta(3)\right)\frac{1}{t} + \left(\frac{122444553407}{726062400000} - \frac{101}{56700}\pi^4 - \frac{7543283}{4375822500}\ln(t)\right. \\
& \left. - \frac{40783}{27783000}\ln^2(t) - \frac{37}{396900}\ln^3(t) - \frac{1}{15120}\ln^4(t) + \frac{37}{33075}\,\zeta(3) - \frac{1}{630}\ln(t)(2-2\zeta(3))\right)\frac{1}{t^2} \\
& + \left[\frac{4252141320359}{66162436200000} - \frac{2}{25515}\pi^4 + \frac{160655261}{88610405625}\ln(t) - \frac{1243103}{1125211500}\ln^2(t) + \frac{1061}{5358150}\ln^3(t)\right. \\
& \left. - \frac{1}{17010}\ln^4(t) - \frac{2122}{893025}\zeta(3) - \frac{4}{2835}\ln(t)\left(\frac{9}{4} - 2\zeta(3)\right)\right]\frac{1}{t^3} \\
& + \left[\frac{415346515794743341}{460318745337675840000} + \frac{47}{1122660}\pi^4 + \frac{53085234133}{16606015344072}\ln(t) - \frac{30820751}{47925008208}\ln^2(t)\right. \\
& \left. + \frac{16783}{51866892}\ln^3(t) - \frac{5}{299376}\ln^4(t) - \frac{16783}{4322241}\zeta(3) - \frac{5}{12474}\ln(t)\left(\frac{251}{108} - 2\zeta(3)\right)\right]\frac{1}{t^4} + \mathcal{O}\left(\frac{1}{t^5}\right). \qquad (29)
\end{aligned}
$$

Figure 5 illustrates that, as in the previous case, the asymptotic expansion $\sim \mathcal{O}(1/r^{10})$ in the right semiplane $r > 1$ approximates the exact corrections $A_2^{(10)}(r)$ quite well at physical values of r, the approximation becoming better with increase of r. This can be clearly seen if one computes again the deviation $\varepsilon(r)$, cf. Eq. (4), in the right semiplane. One has $\varepsilon(r) \simeq 3 \cdot 10^{-6}$ at $r = 16.82$ (corresponds to $\approx m_\tau/m_\mu$) and $\varepsilon(r) \simeq 4 \cdot 10^{-26}$ at $r = 3477.23$ (corresponds $\approx m_\tau/m_e$). This persuades us that likewise in the case $r < 1$, the asymptotic expansion $\sim \mathcal{O}(1/r^{10})$ holds with an amazing accuracy in the whole region of physical values of r and, consequently can be safely applied to compute the tenth order corrections by the simpler formula Eq. (29).

As r decreases further, the deviation $\varepsilon(r)$ increases, becoming rather large, for example, $\varepsilon(r) \sim 32\,\%$ at $r = \sqrt{2}$.

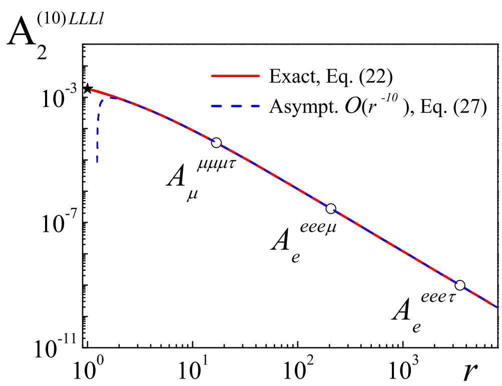

FIG. 5: The tenth order corrections $A_2^{(10)LLL\ell}(r \geq 1)$ in the right semiplane, $r \geq 1$. The solid line is the result of full calculations by Eq. (24), the dashed line corresponds to the asymptotic expansion (29) keeping terms up to $\sim r^8$. The open circles, as well as the associated with them labels, point to the coefficients $A_2^{(10),LLL\ell}(r)$ at r corresponding to physical values of the lepton masses. The star indicates the value of the mass independent coefficient $4A_1^{(10),LLL\ell}(1)$, Eq. (10).

5. Summary

We have presented analytical expressions for the tenth-order QED corrections to the anomalous magnetic moments of leptons due to the diagram with inserts of the vacuum polarization operator consisting of four closed lepton loops, for the case when three of the loops are formed by a lepton L of the same type as the external one, and one loop is formed by a lepton of a different type $\ell \neq L$. This paper is a continuation of our investigations of the corrections to a_L from the "bubble"-like diagrams. As previously, the approach is essentially based on the dispersion relations and the Mellin–Barnes transform for the propagators of massive photons. The method allows one to derive explicitly the corresponding tenth order corrections a_L as functions of the ratio $r = m_\ell/m_L$ of the mass of the internal ℓ to the mass of the external L leptons in the whole interval ($0 < r < \infty$). The resulting expressions turn out to be extremely complicated and cumbersome. However, since in reality for physically existing leptons one has either $r \ll 1$, or $r \gg 1$, it is appropriate to replace the exact expressions by their asymptotic expansions, which are much simpler and more convenient for numerical calculations. The corresponding expansions at $r \ll 1$ and $r \gg 1$ were derived and the limits of their applicability were investigated. We argued that the asymptotic expansions work quite well in the intervals ($0 < r < 0.1$) and ($2 < r < \infty$), and can be safely used for numerical calculations of the coefficient $A_2^{(10)LLL\ell}(r_{phys})$ for each of the charged leptons.

Acknowledgments

This work was supported in part by a grant under the Belarus-JINR scientific collaboration. A bulk of numerical calculations have been performed on the basis of the HybriLIT heterogeneous computing platform (supercomputer "Govorun", LIT, JINR).

References

[1] P. A. M. Dirac, The quantum theory of the electron, Proc. Roy. Soc. Lond. A **117**, 619 (1928).

[2] L. Morel, Z. Yao, P. Clad, S. Guellati-Khelifa, Determination of the fine-structure constant with an accuracy of 81 parts per trillion, Nature **588**, 61-65 (2020).

[3] R. H. Parker, C. Yu, W. Zhong, B. Estey, H. M*ü*eller, Measurement of the fine-structure constant as a test of the Standard Model, Science **360**, 191-195 (2018).

[4] D. P. Aguillard et al. (Muon $g-2$ Collaboration), Measurement of the positive muon anomalous magnetic moment to 0.20 ppm, Phys. Rev. Lett. **131**, 161802 (2023).
Detailed report on the measurement of the positive muon anomalous magnetic moment to 0.20 ppm, Phys. Rev. D **110**, 032009 (2024).

[5] T. Aoyama et al., The anomalous magnetic moment of the muon in the Standard Model, Phys. Rep. **887**, 1-166 (2020).

[6] S. Laporta, High-precision calculation of the 4-loop contribution to the electron $g-2$ in QED, Phys. Letts. **772**, 232-238 (2017).

[7] S. Laporta, High-precision calculation of the 4-loop QED contribution to the slope of the Dirac form factor, Phys. Letts. **800**, 135-137 (2020).

[8] S. Volkov, Calculation of the total 10-th order QED contribution to the lepton magnetic moments, e-Print: arXiv:2404.00649 [hep-ph].

[9] S. Volkov S. Calculation of lepton magnetic moments in quantum electrodynamics: A justification of the flexible divergence elimination method, Phys. Rev. D **109**, 03007 (2024).

[10] D. H. Bailey, D. J. Broadhurst, Parallel integer relation detection: Techniques and applications, Math. Comput. **70**, 1719 (2001).

[11] J. P. Aguilar, D. Greynat, E. de Rafael, Muon anomaly from lepton vacuum polarization and the Mellin–Barnes representation, Phys. Rev. D **77**, 093010 (2008).

[12] E. E. Boos, A. I. Davydychev, A Method of evaluating massive Feynman integrals, Theor. Math. Phys. **89**, 1052-1063 (1991).

[13] I. Dubovyk, J. Gluza, G. Somogyi, Mellin–Barnes Integrals: A Primer on Particle Physics Applications, Lect. Notes Phys. **1008**, 1-208 (2022).

[14] V. A. Smirnov, Analytic tools for Feynman integrals, Springer Tracts in Modern Physics **250**, 1-296 (2012).

[15] A. V. Kotikov, S. Teber, Multi-loop techniques for massless Feynman diagram calculations, Phys. Part. Nucl. **50**(1), 1-41 (2019).

[16] O. P. Solovtsova, V. I. Lashkevich, L. P. Kaptari, Lepton anomaly from QED diagrams with vacuum polarization insertions within the Mellin– Barnes representation, Eur. Phys. J. Plus **138**, 212 (2023).

[17] O. P. Solovtsova, V. I. Lashkevich, L. P. Kaptari, Contributions of QED diagrams with vacuum polarization insertions to the lepton anomaly within the Mellin–Barnes representation, Phys. Part. Nucl. **55**, 725-730 (2024).

[18] O. P. Solovtsova, V. I. Lashkevich, L. P. Kaptari, Analytical calculations of the tenth order QED radiative corrections to lepton anomalies within the Mellin–Barnes representation, Journal of Physics G: Nuclear and Particle Physics **51**, 055001 (2024).

[19] O. P. Solovtsova, V. I. Lashkevich, L. P. Kaptari, Radiative QED corrections to the lepton anomaly from four-loop vacuum polarization insertions with three identical leptons, e-Print: arXiv:2406.16645[hep-ph].

[20] B. E. Lautrup, E. de Rafael, Calculation of the sixth-order contribution from the fourth-order vacuum polarization to the difference of the anomalous magnetic moments of muon and electron, Phys. Rev. **174**, 1835-1842 (1968).

[21] J. S. Schwinger, On quantum electrodynamics and the magnetic moment of the electron, Phys. Rev. **73**, 416 (1948);
Quantum electrodynamics. III: The electromagnetic properties of the electron: radiative corrections to scattering. Physical Review **76**, 790-817 (1949).

[22] B. E. Lautrup, On high order estimates in QED, Physical Letter B **69**, 109-111 (1977).

[23] M. L. Laursen, M. A. Samuel, The n-bubble diagram contribution to $g - 2$ of the electron mathematical structure of the analytical expression, Phys. Letts. **91B**, 249-252 (1980).

[24] A. V. Sidorov, V. I. Lashkevich, O. P. Solovtsova, On the contribution of muon loops to the anomalous magnetic moment of the muon, Int. J. Nonlin. Phenom. Complex Syst. **21**(4), 395-401 (2018).

[25] E. Tiesinga, P. J. Mohr, D. B. Newell, B. N. Taylor, “CODATA recommended values of the fundamental physical constants: 2018,” Rev. Mod. Phys. **93** no.2, 025010-46 (2021).